BI-DIRECTIONAL REFLECTANCE MEASUREMENT OF PULSE-LASER IRRADIATED AIRLESS BODY ANALOG MATERIALS. Te Jiang[1], Hao Zhang[1], Yazhou Yang[1], Pei Ma[1], Xiaoyi Hu[1], and Yuxue Sun[1], China University of Geosciences, Wuhan, China. tejiang@cug.edu.cn

Introduction: Space weathering processes including solar wind irradiation and micrometeorite bombardment produce nano-phase iron (*npFe^0*) and amorphous layers that redden and darken the visible and near-infrared (VNIR) reflectance spectra of the surface of airless bodies. The ability that how a surface would send light into different directions can be quantitatively described by the bi-directional reflectance distribution function (***BRDF***) [1]. The *BRDF* of an airless body is closely related to the physical properties of the surface regolith such as particle size distribution, refractive indices, and porosity [1, 2]. To understand how Space weathering may change the directional reflectance properties of regolith layers, we carried out pulsed laser irradiation experiments on olivine (OL), orthopyroxene (OPX), anorthosite (AN), ilmenite (ILM), and JSC-1A Lunar Regolith Simulant (LRS), and measured their spectral reflectance and *BRDF*. Here we present the *BRDF* and radiative transfer modeling results.

Samples and Experiments: The four pure minerals: OL, OPX, AN, and ILM, are typical minerals found on surfaces of the Moon and some S-type asteroids. The JSC-1A LRS (from Orbitech) mainly consists of the above four minerals. All samples were ground and sieved to <45 μm but the unsieved JSC-1A (< 1 mm) was also used. Our micrometeorite bombardment simulation system [3] includes a 1064 nm Nd: YAG pulsed laser with a pulse width of 6-8 nanoseconds and a vacuum chamber installed on a motorized two-dimensional translation stage. Before irradiation takes place, the chamber was pumped down to $3*10^{-3}$ Pa or lower. Different pulse-laser energy density level combinations (50 mJ*2, 4, and 6 times) were used to simulate micrometeorite bombardment with different impact energies (**Fig. 1**).

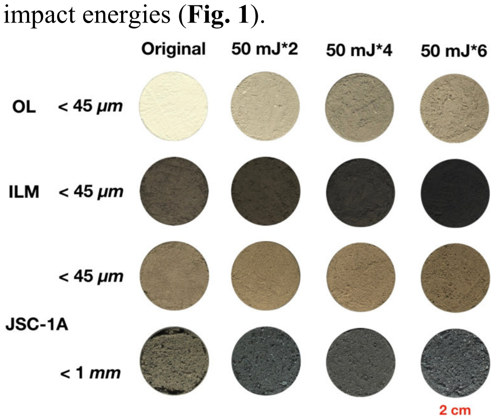

Fig. 1: Photos of the original and pulse-laser irradiated samples.

The VNIR and mid-infrared (MIR) reflectance spectra (0.5~25 μm) of the original and irradiated samples were measured with a Bruker Vertex 70 FTIR spectrometer. A custom made goniometer was used to measure the BRDF and polarization of the samples at 633 nm [4]. The minimum phase angle of the system is 2.7° and with an incident zenith angle of 60° the maximum phase angle is 130°. The *BRDF* of all samples were measured with a 3° step. **Fig. 2** shows the *BRDF* of the original and 50 mJ*6 irradiated samples.

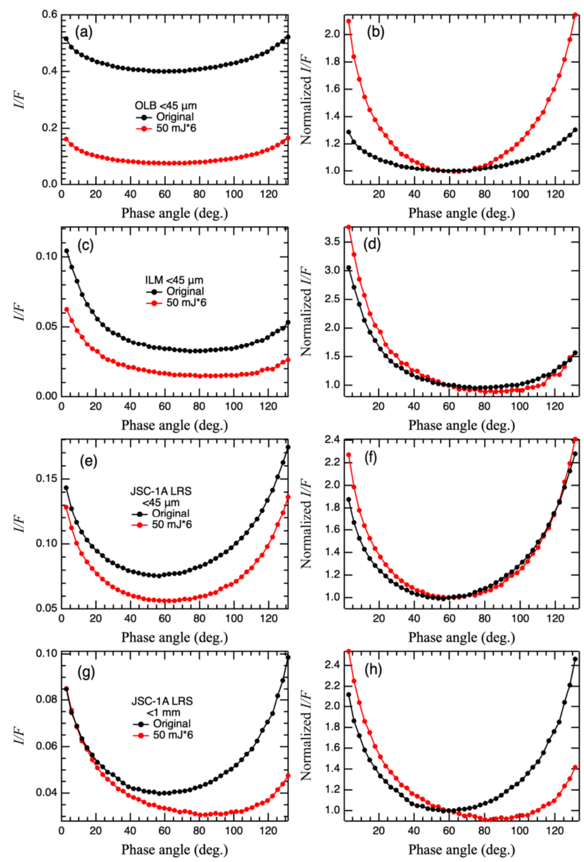

Fig. 2: Radiance Factor (*I/F*) (**a, c, e, g**) and normalized *I/F* (**b, d, f, h**) of OL, ILM, JSC-1A LRS <45 μm and <1 mm. *I/F* is normalized at 60° phase angle.

Results:

Reflectance spectra. Reflectance spectra from visible to mid-infrared (0.5-25 μm) of OL, ILM and

JSC-1A LRS <45 μm grains show significant darkening and reddening in the VNIR region but insignificant changes in the MIR region, consistent with our previous simulation results on OL [3]. In contrast, the JSC-1A LRS with size distribution <1 mm shows spectral bluing in the visible after irradiations. From the Transmission Electron Microscope images, the pulse-laser successfully produced *npFe* and amorphous layers [3]. Magnetic measurements have demonstrated that at least a large portion of the iron grains are *npFe*^{0}. The results for OPX and AN are similar to that of the OL and thus are not shown here.

BRDF. Upon irradiation, the BRDF values of the samples decrease and the normalized (at 60º phase angle) ones have both enhanced back- and forward-scattering components for OL. For the other three samples, all have enhanced backscattering but decreased (ILM and JSC-1A < 1 mm) or nearly unchanged (JSC-1A <45 μm) forward scattering (**Fig. 2**).

Numerical radiative transfer calculations: Using OL as an example, numerical radiative transfer computations [5] were used to calculate the *BRDF* of OL grains with *npFe*^{0} (0 wt %, 0.01 wt %, 0.1 wt %, 1 wt %) uniformly distributed inside the grains. The results show that OL with higher concentrations of *npFe*^{0} have lower absolute *BRDF* values (**Fig.3a**) and enhanced back- and forward scattering components (**Fig. 3b**), consistent with measurement results of OL (**Figs. 2a and 2b**).

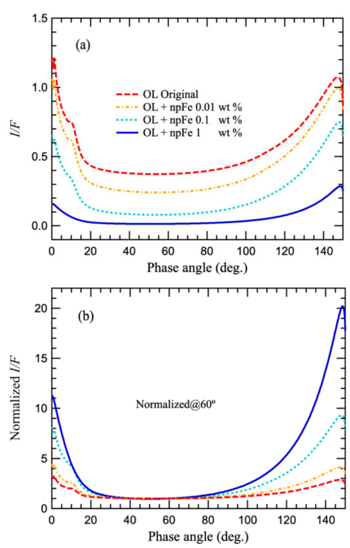

Fig.3: *I/F* (a) and normalized *I/F* (b) of the original OL and OL with varied concentrations of *npFe*^{0} (wt: 0.01 %, 0.1%, 1%) uniformly distributed inside the grains.

We also calculated OL grains coated with various coating thicknesses (50~1000 nm) and various *npFe*^{0} weight percentages by using the BART code [6]. The results show the the absolute *BRDF* decrease and the normalized BRDF have both enhanced back- and forward scattering lobes as the coating thickness increases, consistent the measurement results.

Hapke model fitting: To understand the changes in single scattering before and after irradiations, a 5-parameter Hapke model (ω, b, c, B_{S0}, hs) [1] was used to fit the *BRDF* and a grid-search was performed to find the most probable fitting parameters. **Fig. 4** shows the fitted 2-term Henyey-Greenstein phase functions for the four samples. One can see that compared with the original ones, all sample grains become more backscattering (with smaller asymmetry parameters, ξ=-bc) upon the strongest irradiation.

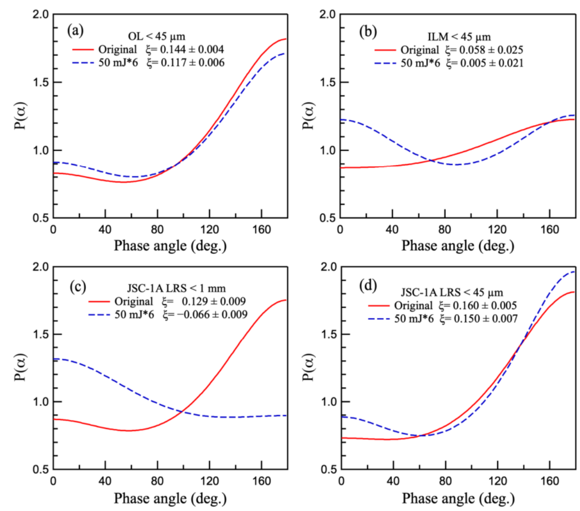

Fig. 4: Fitted 2-term Henyey-Greenstein phase functions of the 4 original samples and that of the samples irradiated with the strongest irradiations (50 mJ*6 times). The asymmetry parameter ξ for each sample is shown in each plot.

Conclusion: These results indicate that the directional reflectance properties of space weathered regolith grains of airless bodies may be more backscattering than that of fresh materials, see [7] for more details. However, the decreased forward scattering for ILM and JSC-1A <1 mm remains unexplained . Measurements and modeling on more samples with different size distributions and more mineral mixtures are expected in future.

References:

[1] Hapke B. (2012), Theory of Refl. & Emitt. Spectroscopy. [2] Shkuratov Y. et al. (2011) *PSS,* 59, 1326-1371. [3] Yang Y. et al. (2017) *A&A* 597, A50. [4] Zhang H. et al. (2014) *45th LPSC* abstract#1777. [5] Mishchenko M. I. et al. (2015) *JQSRT,* 156, 97-108. [6] Quirantes, A., and Delgado A. V. (1997) *J Phys. D Appl. Phys.,* 30, 2123. [7] Jiang T. et al. submitted to *Icarus*.